Exploring estuarine eutrophication sensitivity to nutrient loading

Mary Anne Evans,[a,1,*] and Donald Scavia [a,b]

[a] School of Natural Resources and Environment, University of Michigan, Ann Arbor, Michigan
[b] Graham Environmental Sustainability Institute, University of Michigan, Ann Arbor, Michigan

Abstract

The sensitivity of surface chlorophyll (Chl) and bottom water dissolved oxygen (DO) to total nitrogen (TN) load was investigated using a Bayesian-based process model fit to data from a range of estuaries. The model was used to test if the sensitivity of DO depletion to TN loads is dependent only on factors controlling the sensitivity of surface Chl, or if additional factors are important. Results indicate that separate processes control Chl and DO sensitivity, and that these sensitivities vary among estuaries. Analysis of fitted parameters across estuaries showed that Chl sensitivity to TN loading was positively correlated with water residence time, and DO sensitivity to Chl was positively correlated with relative mixing depth.

Ecosystem sensitivity to external stressors and the biophysical control of this sensitivity have long been of interest to ecologists. Recent work has focused on the combined effects of multiple stressors and on the relative sensitivity of ecosystem functions (Blake and Duffy 2010; Wiley et al. 2010). Many open questions remain in both of these areas. In this study, we explored factors controlling the relative sensitivity of chlorophyll (Chl) concentration and bottom water dissolved oxygen (DO) depletion to nutrient stress across estuaries.

Because of a convergence of freshwater and saltwater habitats, their association with high human population densities, and their semi-enclosed nature, estuaries are highly sensitive to loads of nutrients, sediment, and toxins and are excellent study systems for exploring questions of sensitivity. Nutrient overfertilization has led to significant eutrophication in many systems (Bricker et al. 2007), and that is the subject of this study.

Nutrient fertilization of coastal waters causes both primary and secondary symptoms of eutrophication. Primary symptoms include increases in Chl and primary production, changes in nutrient ratios, increased sedimentation of organic carbon, and changes in phytoplankton species composition. These changes can cascade into secondary symptoms, including changes in water transparency, decreases in bottom water DO, animal mortality or displacement, shading or toxic inhibition of submerged aquatic vegetation, and many others (Cloern 2001). Here we focus on two key symptoms, increased Chl concentration and decreased bottom water DO, because of their ecological importance and management attention.

Increases in phytoplankton biomass, often represented as Chl concentration, are the most commonly reported symptoms of eutrophication in estuaries and are a key precursor to many of the secondary symptoms (Cloern 2001). Sinking and decomposition of phytoplankton biomass are major drivers of DO depletion. DO depletion

can lead to widespread ecosystem changes, including fish kills (Diaz and Rosenberg 2008), decreased or displaced fish production (Rabalais and Turner 2001), altered biogeochemical cycles (Turner et al. 2008), and decreased societal value through reduced recreational opportunities and fisheries harvest losses (Renaud 1986). The issue has become widespread worldwide (Diaz and Rosenberg 2008; Zhang et al. 2010).

Clear links exist between nutrient loads, especially total nitrogen (TN), and bottom water DO, for example, in the Gulf of Mexico (Turner et al. 2008; Greene et al. 2009) and in Chesapeake Bay (Kemp et al. 2005; Liu and Scavia 2010). However, the sensitivity of bottom water DO to TN loading has also been shown to vary through time (Liu and Scavia 2010; Liu et al. 2010; Scully 2010) and among estuaries (Zhang et al. 2010). Here, we expand on these analyses to explore the relative simultaneous sensitivity of Chl concentration and DO depletion to TN loading in a cross-estuary context.

Estuarine eutrophication sensitivity to TN loading is modulated through ecological filters, system-specific processes that modulate responses to enrichment (Cloern 2001). These filters include the degree of tidal flushing and turbulent mixing that can dilute TN loads and reduce eutrophication symptoms (Monbet 1992; Cloern 2001); the degree of freshwater flushing and residence time, which determine the time during which nutrients are available for estuary processing (Swaney et al. 2008; Steward and Lowe 2010); and biological factors such as top-down control of phytoplankton biomass (Cloern 2001).

As part of a toolbox for eutrophication filter evaluation, a mechanistic estuarine model of TN-driven surface-layer Chl concentration has been tested and is available (Scavia and Liu 2009). We expand that model to a two-layer version that includes surface Chl and bottom-layer organic carbon and DO. The model was constructed and fit using Bayesian inference based on seasonally and spatially averaged, satellite-derived Chl estimates used in Scavia and Liu (2009) and summer average, bottom water DO data from the National Estuarine Eutrophication Assessment (NEEA; Bricker et al. 1999, 2007). We used the model to test if the sensitivity of DO depletion to TN loads is

---

* Corresponding author: mevans@umich.edu

[1] Present address: U.S. Geological Survey, Great Lakes Science Center, Ann Arbor, Michigan

Table 1. Estuary names and locations.

U.S. estuaries	Longitude (°W)	Latitude (°N)
Buzzards Bay, MA	70.84053	41.59181
Willapa Bay, WA	123.96941	46.55985
Choctawhatchee Bay, FL	86.3161	30.4474
Pensacola Bay, FL	86.96511	30.46379
Patuxent River, MD	76.51213	38.38493
Potomac River, MD/VA	77.09428	38.39602
Central San Francisco Bay, CA	121.96481	38.18366
Neuse River, NC	76.57693	35.03501
Winyah Bay, SC	79.25778	33.39368
Charleston Harbor, SC	79.95033	32.90534
St. Helena Sound, SC	80.39301	32.53613
Broad River, SC	80.71693	32.39863
Savannah River, GA	80.93814	32.1364
St. Marys River and Cumberland Sound, GA/FL	81.4844	30.75114
Blue Hill Bay, ME	68.45747	44.34721
Penobscot Bay, ME	68.86359	44.40772
Casco Bay, ME	70.07362	43.75061

dependent only on factors that control the sensitivity of surface Chl concentration, or if additional factors control sensitivity of DO to Chl.

Methods

Data sources—Data on estuary depth, volume, water residence time, TN load, summer surface Chl concentration, freshwater discharge, precipitation and evaporation at the estuary surface, estuary and ocean boundary salinity, and ocean boundary nitrogen concentration were obtained and used as described in Scavia and Liu (2009) from the NEEA Estuaries Database (http://ian.umces.edu/neea; Bricker et al. 2007), Sea-viewing Wide Field-of-View Sensor (SeaWiFS) imagery (http://geoportal.kgs.ku.edu/estuary/; Hooker and Firestone 2003), and the U.S. Geological Survey spatially referenced regressions on watershed attributes (SPARROW) model (Alexander et al. 2008; R. Alexander pers. comm.). SPARROW loads are annual averages that incorporate weather conditions for 10 yr periods centered on agricultural census years; we used the SPARROW loads for the agricultural census year 1992. Of the 75 U.S. estuaries for which Chl was modeled in Scavia and Liu (2009), we used the 17 (Table 1) that stratify seasonally or longer and for which DO data are available to test the current model. These include 2 lagoons, 2 coastal embayments, 3 fjords, and 10 river-dominated estuaries, with broad ranges of maximum depth (8–149 m), volume (2.1–244.0 × 10^8 m^3), freshwater inflow (4.2–723.0 × 10^5 m^3 d^{-1}), water residence time (5–468 d), average water temperature (7.2–20.7°C), TN loading (5.5–684.0 × 10^5 kg yr^{-1}), average summer Chl (2.6–24.0 µg L^{-1}), and average bottom water DO (0.9–9.5 mg O_2 L^{-1}).

Average summer bottom-layer DO concentration, as well as average estuary and ocean boundary temperatures were obtained from the NEEA Estuaries Database (http://ian.umces.edu/neea; Bricker et al. 2007). This database was compiled through local expert elicitation for each system, asking experts to provide estimates of average summer bottom-layer DO concentration along with their level of

confidence in this estimate. We used only systems where the respondents reported "high confidence" in the DO values; however, given the nature of the survey, there are likely some inconsistencies among estuaries in the data collection and "averaging" methods. Estuary surface layer and ocean boundary DO concentrations were assumed to be saturated and were calculated from the temperature and salinity of each water body using the following formula, which is applicable over the range −1°C to 40°C and 0 to 40 g kg^{-1} salinity (Weiss 1970; Hull et al. 2008):

$$O_i = 14.62 - 0.37T_i + 0.0045T_i^2 \\ - 0.097S_i + 0.00205T_iS_i + 0.0002739S_i^2 \tag{1}$$

where $i = 1$ for the estuary surface layer and o for the ocean boundary; O_i = concentration of DO at saturation (mg L^{-1}), T_i = temperature (°C), and S_i = salinity (g kg^{-1}).

Model development—Modeled estuaries were assumed to be horizontally well mixed and vertically stratified in two layers due to salinity–density differences. Phytoplankton, detritus, and oxygen (PDO) were modeled for each layer based on a mass balance with river and ocean import, ocean export, and nutrient-driven production (Fig. 1). Ocean import and export were based on water balances and concentrations in the source water. The following equations were used for all lagoons, coastal embayments, and river-dominated estuaries. For fjords, the input terms were modified such that oceanic inputs were into the upper rather than the lower layer.

Surface-layer phytoplankton biomass (*B*), TN-driven biomass production, grazing, sinking, thickness, and volume of each estuary layer, and estuary water residence time (WRT) were all modeled as in Scavia and Liu (2009). Primary production was estimated by converting TN load to organic carbon production based on Redfield ratios (Scavia et al. 2006). Planktonic N fixation was not included because it is generally not observed in estuaries with salinities more than 10 to 12, even when they are strongly N limited (Howarth and Marino 2006). The surface-layer
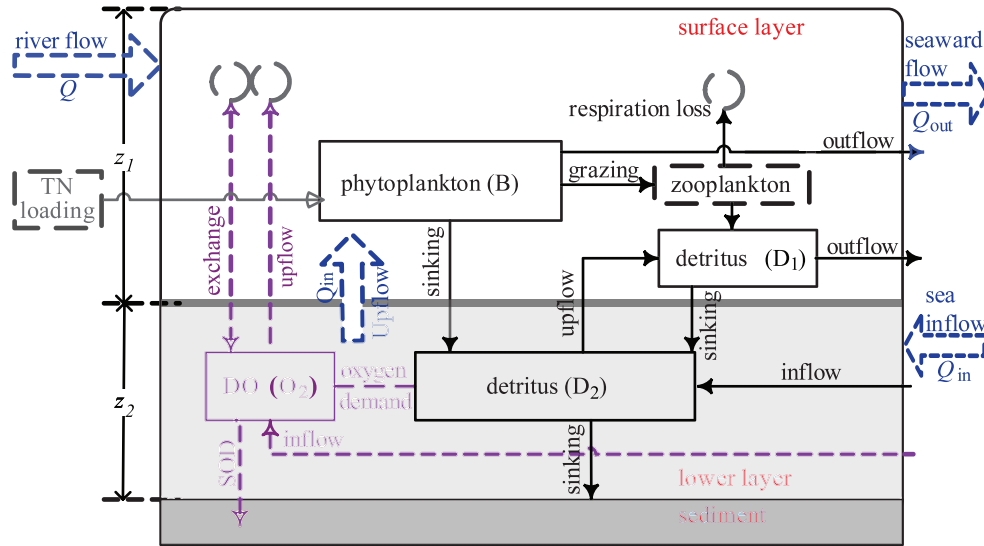
Fig. 1. Diagram of model state variables and processes for a stratified, non-fjord estuary. In fjords, the sea inflow is switched to the upper layer.

biomass model included an estuary-specific term (α) that is proportional to the estuary's efficiency at converting TN loads to phytoplankton biomass. Scavia and Liu (2009) showed that this term can be used as an indicator of estuary Chl sensitivity to TN load.

Detritus in the surface layer (mg C L^{-1}) was modeled as a function of grazing inefficiency (biomass consumed but not respired by grazers), decomposition in the surface layer, loss to the ocean, upwelling from the lower layer, and sinking. Grazing was modeled as a quadratic term of phytoplankton biomass assuming zooplankton biomass is proportional to phytoplankton biomass (Scavia and Liu 2009).

$$\frac{dD_1}{dt} = LB^2a - k_mD_1 - \frac{Q_{out}D_1}{V_1} + \frac{Q_{in}D_2}{V_1} - v'_{s1}D_1 \quad (2)$$

where D_1 is detritus in the surface layer (mg L^{-1}); L is the rate of loss to grazing by zooplankton (d^{-1}); B is phytoplankton biomass (mg L^{-1}); a is the fraction of zooplankton grazing converted to detritus; k_m is the mineralization rate (d^{-1}); Q_{out} is the outflow to the ocean ($m^3\ d^{-1}$); V is the estuary volume (m^3) with V_1 for the surface and V_2 for the bottom layer ($V = V_1 + V_2$); Q_{in} is the oceanic inflow ($m^3\ d^{-1}$), representing upwelled bottom water into the surface layer; D_2 is detritus in the bottom layer (mg L^{-1}), $v'_{s1} = v_s/z_1$ is the sinking rate of phytoplankton from the surface layer (d^{-1}), calculated as the sinking speed (v_s, m d^{-1}) over layer depth; and z_1 is the estuary average depth (m) of the surface layer. Total estuary average depth z (m) $= z_1 + z_2$, where z_2 is the depth of the bottom layer.

Detritus in the lower layer (D_2, mg C L^{-1}) was modeled as a function of sinking of detritus and biomass from the surface layer, inflow from the ocean, decomposition, and upwelling losses to the surface layer.

$$\frac{dD_2}{dt} = \frac{v'_{s1}V_1}{V_2}(D_1 + B) + \frac{Q_{in}B_o}{V_2} - k_mD_2 - \frac{Q_{in}D_2}{V_2} - v'_{s2}D_2 \quad (3)$$

where B_o is the concentration of organic matter in the ocean (mg C L^{-1}), and $v'_{s2} = v_s/z_2$ is the sinking rate of

phytoplankton from the bottom layer (d^{-1}), calculated as the sinking speed (v_s, m d^{-1}) over layer depth.

Oxygen in the lower layer (mg L^{-1}) was modeled as a function of mixing from the surface layer, upwelling loss to the surface layer, gain from the ocean, decomposition, and sediment respiration.

$$\frac{dO_2}{dt} = k_d(O_1 - O_2) - \frac{Q_{in}O_2}{V_2} + \frac{Q_{in}O_o}{V_2} - k_mD_2k_r - v'_{s2}k_rD_2 \quad (4)$$

where O_2 is the oxygen concentration in the lower layer (mg L^{-1}); k_r is the respiratory quotient (3.49 g O_2 consumed per g C respired, including both C→CO_2 and NH_4→NO_3 pathways; Chapra 1997); k_d is the exchange coefficient between the two layers (d^{-1}); and the final term ($v'_{s2}k_rD_2$) is the areal rate of sediment oxygen demand (SOD, g $O_2\ m^{-2}\ d^{-1}$). This final term assumed that the sediments are in equilibrium with respect to carbon flux, and thus SOD was approximated by carbon deposition to the sediment surface.

Analytical steady-state solutions—We used steady-state solutions for the previous differential equations because temporally varying TN load and DO data were not available for most of the estuaries we modeled. While this is a significant simplifying assumption, it is supported by the fact that variability among systems is higher than within systems and that there are relatively small temporal trends in chlorophyll or TN loads for these systems. Thus, the steady-state approximation was reasonable for drawing distinctions among estuaries (Dettmann 2001; Fennel and Boss 2003; Swaney et al. 2008).

The steady-state solutions for surface-layer biomass (from Scavia and Liu 2009) are

$$B = \frac{-(Q_{out} + V_1v'_{s1}) + \sqrt{(Q_{out} + V_1v'_{s1})^2 + 4I_nLV_1^2}}{2LV_1} \quad (5)$$

and

$$I_n = \alpha \frac{TN_R + TN_O}{V_1} \quad (6)$$

where I_n is primary production, α is a scaling coefficient including the Redfield C:N ratio and estuary efficiency, and TN_R and TN_O are total nitrogen inputs from river and ocean sources, respectively.

The steady-state solutions for the detritus and oxygen equations (Eqs. 2–4) are:

$$D_1 = \frac{B_o Q_{in}^2 + BV_1\{v'_{s1}Q_{in} + aBL[Q_{in} + V_2(k_m + v'_{s2})]\}}{Q_{in}(Q_{out} + k_m V_1) + V_2(k_m + v'_{s1})[Q_{out} + V_1(k_m + v'_{s1})]} \quad (7)$$

$$D_2 =$$

$$\frac{B_o Q_{in}[Q_{out} + V_1(k_m + v'_{s1})] + BV_1 v'_{s1}[Q_{out} + V_1(k_m + aBL + v'_{s1})]}{Q_{in}(Q_{out} + k_m V_1) + V_2(k_m + v'_{s1})[Q_{out} + V_1(k_m + v'_{s1})]} \quad (8)$$

$$O_2 = \frac{k_d O_1 + \frac{Q_{in}O_O}{V_2} - k_m k_r D_2 - v'_{s2} k_r D_2}{\frac{Q_{in}}{V_2} + k_d} \quad (9)$$

Finally, we defined a parameter f_z as the ratio of surface-layer to total volume (unitless):

$$f_z = \frac{z_1}{z_{max}} = \frac{V_1}{V} \quad (10)$$

Parameter estimation—The model was simultaneously fit to NEEA summer average bottom water oxygen concentration estimates and 7 yr (1998–2004) of summer average surface-layer Chl concentrations using a constant carbon to Chl ratio (ca) to convert phytoplankton biomass (B) to units of Chl (Scavia and Liu 2009). For some tests, we treated α and f_z as variable among estuaries (full model), using a hierarchical structure for α, as described in the following. We compared these results to estimations with each parameter fit as constant across estuaries. Estuary-specific calibration parameters serve as an index of estuary sensitivity of Chl (α) and DO (f_z) to TN load.

Model estimation was done through Markov chain Monte Carlo (MCMC) with Gibbs sampling methods for Bayesian inference in WinBUGS (version 1.4.3; Lunn et al. 2000) called from R (version 2.6.0; R2WinBUGS, version 2.1–8; Gelman and Hill 2007). Model code for both R and WinBUGS is available from the authors. All parameters were fit as distributions with variability propagated by the MCMC process. Fitting to observed values was done to minimize variance (σ^2_{Chl} and σ^2_{DO}) in the following distributions:

$$Chl(obs)_i \sim N(B \times ca, \sigma^2_{Chl}) \quad (11)$$

where $i = 1, ..., 7$ for the 7 yr of Chl data, and

$$DO(obs) \sim N(O_2, \sigma^2_{DO}) \quad (12)$$

where N indicates a normal distribution, and the values in parentheses are average and variance.

MCMC algorithms were run for 10,000 iterations (first 5000 discarded) using four chains, or parallel runs using different random seeds, to test for model convergence. Model convergence was tested using the ratio between: within chain variance, $\hat{R}$. At convergence, $\hat{R} \approx 1$ (Gelman and Hill 2007), and model runs with $\hat{R} > 1.2$ were not used for analysis. Marginal distributions for each parameter were drawn from 1000 MCMC samples for each parameter after thinning to reduce serial correlation (Qian et al. 2003; Malve and Qian 2006). The following uninformative priors were used: (1) in calibrations with α varying by estuary ($n = 1$ through 17) with a hierarchical structure $\alpha_n \sim N(\alpha^*, 1000)I(0.00001, 200)$ and $\alpha^* \sim Uni(0.0001, 200)$; (2) in calibrations with α constant across estuaries, the same prior as α_n; (3) in calibrations with f_z varying by estuary ($n = 1$ through 17) $f_{zn} \sim Uni(0.05, 0.95)$; and (4) in calibrations with f_z constant across estuaries, the same prior as f_{zn}. Here, N indicates a normal distribution, and Uni indicates a uniform distribution, the values in the first parentheses are average and variance (σ^2) (normal distribution) or upper and lower bounds (uniform distribution), and I(#,#) denotes truncation to remove values outside the range specified. Uninformative truncation at values far outside the expected range (i.e., 0.00001, 200) was conducted to speed conversion and give sensible results. When α was allowed to vary by estuary, it was given a hierarchical structure with the universal mean value (α^*), and α_n and f_{zn} were drawn independently for each estuary.

Values for the remaining parameters were estimated from the literature, or otherwise reasonable values, as described next. The mineralization rate k_m was set to 0.8 d^{-1}, the carbon to Chl ratio (ca) was set to 50 g C:1 g Chl (Riemann et al. 1989), zooplankton grazing rate (L) was set to 0.2 d^{-1}, the fraction of zooplankton grazing converted to detritus (a) was set to 0.2, sinking rate (v_s) was set to 1 m d^{-1} (Lucas et al. 1998), the exchange coefficient between the two layers (k_d) was set to 0.2 d^{-1}, and the concentration of organic matter in the ocean (B_o) was set to 0.3 mg L^{-1}. The initial test, using a range of parameter values, showed that the model was relatively insensitive within these ranges, with the exception of k_d. Parameters were perturbed, one by one, by up to $\pm20\%$, and in all cases, model fit (deviance) changed by a much smaller percent than the parameter change. The value for k_d can vary by more than an order of magnitude in observations and model studies (Borsuk et al. 2001; Liu et al. 2010), so we tested this parameter over a larger range than the others. Our analysis indicated that model fit deteriorates at the lower end of the observed range (values less than 0.1), so we selected a k_d value within the range where model fit was less sensitive to this parameter.

Model fit was determined by comparing observations with the model 95% credible intervals (CI) and by regressions of model results (average of the distribution) vs. observed values (Scavia and Liu 2009). Posterior *P*-values were calculated for each Chl and DO prediction, and *P*-value histograms were used to compare model fit (Gelman et al. 1996; Gronewold et al. 2009).

Tests of DO depletion sensitivity to TN load—We used the model to test if the sensitivity of DO depletion to TN
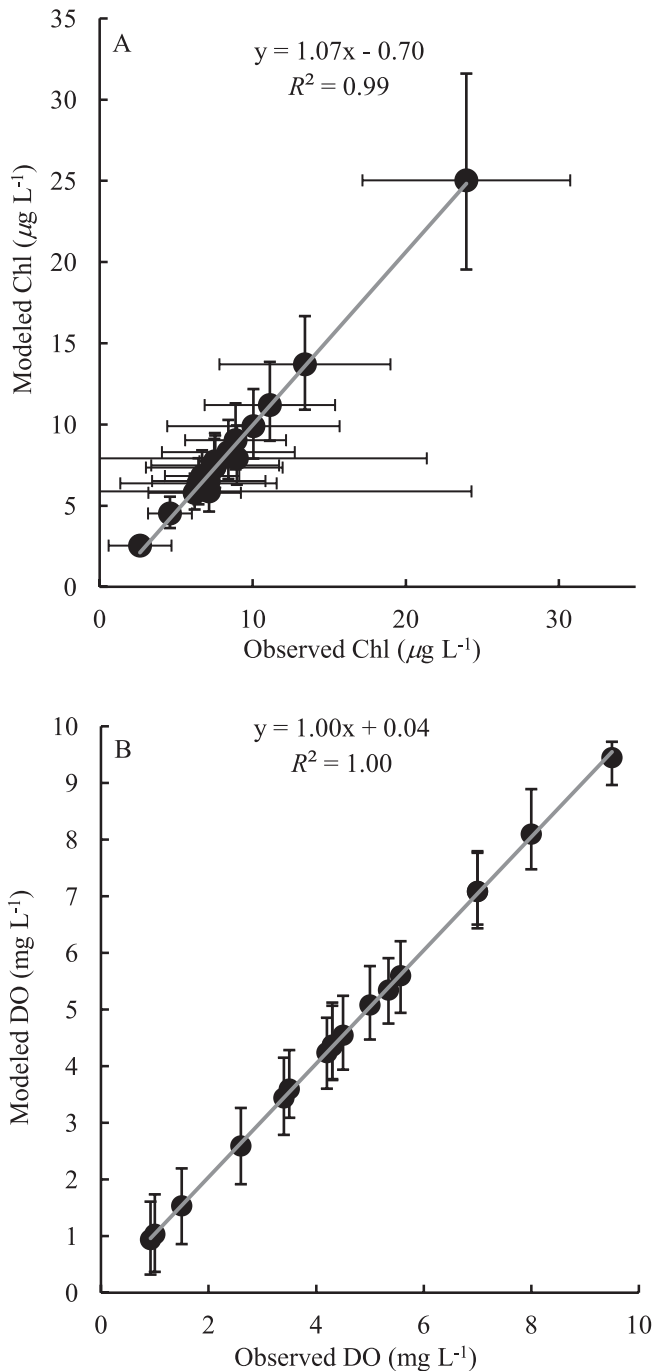
Fig. 2. Model fit for (A) Chl and (B) DO with 95% CI error bars for model predictions and Chl measurements, and parameters α and f_z allowed to vary by estuary (fitted and predicted using 1992 SPARROW loads). Regressions of predicted vs. observed are given to summarize model fit; these were calculated using the mean values for each estuary.

loads is dependent only on factors that control the sensitivity of surface Chl concentrations, or if additional factors are important. Models fit with either α or f_z, as an estuary-specific calibration (the other estimated as constant across estuaries), were compared to models that allowed both parameters to vary by estuary. In all cases, α was tested in the range 0.0001 to 200, and f_z was tested in the

range 0.05 to 0.95. If the sensitivity of DO to TN loads is strictly dependent on factors controlling the sensitivity of surface Chl concentrations, then a single calibration parameter should be sufficient to fit most of the variation in both Chl and DO. However, if additional factors are important, then allowing both parameters to differ among estuaries should be necessary to achieve an adequate fit. The Deviance Information Criterion (DIC) was used to test model fit (Spiegelhalter et al. 2002). Models with the lowest DIC were selected as having better fit, with DIC differences of more than 3 units assumed to indicate strong support for the model with the lower DIC (Spiegelhalter et al. 2002). In addition, we employed a heuristic criterion, asking if one of the simpler models provided an adequate fit, as further discussed in the results. We further tested the independence of the controls on sensitivity of Chl and DO to TN loading by checking for cross-estuary correlations between the fitting parameters α and f_z.

Results

Allowing both α and f_z to differ among estuaries was necessary to achieve an adequate fit to the data; however, this method tended to overfit the DO observations. When calibrated in this way, the model provided an excellent fit ($R^2 > 0.99$, slope ~ 1, and all observations were within the model 95% CI) to both the average Chl data (Fig. 2A) and the DO data (Fig. 2B), and there was no significant correlation between α and f_z ($R^2 = 0.06$; Fig. 3). Posterior P-value histograms show a slight overfitting of Chl and DO. Total DIC was 79.17. When only α was allowed to differ among estuaries, model fit was reduced (Fig. 4; $R^2 = 0.67$ for Chl and 0.81 for DO). More critically, the model was not able to reproduce the observed range of Chl values (slope of observed vs. modeled regression = 0.45), and many observations were outside the 95% (Fig. 4). Posterior P-values indicate that the model severely underfit the DO observations. Total DIC was 241.806, indicating that the model allowing only α to differ among estuaries was a much poorer fit despite the difference in number of parameters. When only f_z was allowed to differ among estuaries, fitting procedures failed to converge on a solution. From this, we conclude that separate processes likely control the dominant sensitivity of Chl concentration and DO depletion to TN loading. Therefore, all remaining analysis examined the model fit allowing both α and f_z to differ among estuaries.

The parameter for Chl conversion efficiency (α), and its variation among estuaries, was similar to that found by Liu and Scavia (2010), despite the model changes made to incorporate DO (Fig. 5; slope = 1.2, intercept = 0.09, $R^2 = 0.92$), suggesting a robust modeling framework.

Before conducting our exploration of the role of the physical filters in controlling estuarine sensitivity, we compared modeled process rates to empirical estimates, when available, because it is possible to match observed state variables with erroneous but compensating process rates. Observed rates of vertical DO flux for Chesapeake Bay (0.1–0.3 g m^{-3} d^{-1}; Kemp et al. 1997; Scavia et al. 2006) fell at the lower end of our modeled means (0.12–1.7 g m^{-3} d^{-1}),
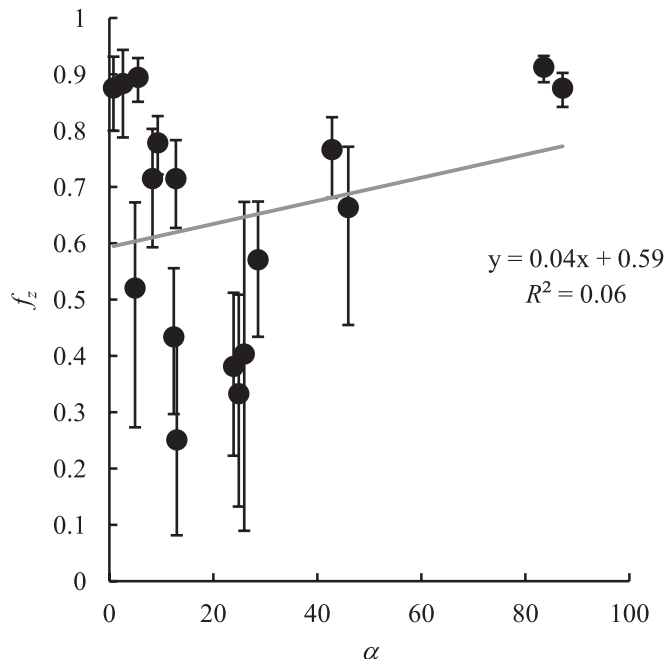
Fig. 3. Calibration parameters for estuary TN to Chl conversion efficiency (α) and relative mixing depth (f_z). Dots are mean values, and error bars are 95% CI.

and the Hopkins River, an Australian estuary, (0.1–1.4 g m^{-3} d^{-1}; Sharples et al. 2003) spans most of the range of modeled fluxes; however, vertical DO flux in Mobile Bay (4.1–4.6 g m^{-3} d^{-1}; Park et al. 2007) exceeded model estimates.

In general, our modeled respiration rates fell within, but at the low end of, expected ranges. Respiration rates (g m^{-3} d^{-1}) for Pensacola Bay (0.32) and Patuxent River Estuary (0.25–0.50; Murrell et al. 2009) overlapped or spanned the modeled 95% CI (0.23–0.32). In addition, measured rates for Chesapeake Bay (0.5–0.7; Kemp et al. 1997; Scavia et al. 2006) span modeled rates (0.21–0.63) for its tributary estuaries, and rates for South San Francisco Bay (0.00–0.9; Caffrey et al. 1998) span modeled rates for Central San Francisco Bay (0.14–0.21). Higher respiration rates have also been observed in Mobile Bay (0–3.7; Park et al. 2007), Hopkins River Estuary (mean 6.5; Sharples et al. 2003), and the Swan River Estuary (mean 2.9; Atkinson et al. 1987).

Comparison of our estimated relative mixing depth (f_z) to observations is more complicated because the model assumes estuaries with flat bottoms, and thus relative mixing depth and relative mixing volume in the model are the same. However, we can test our estimates of relative mixing depth because relative mixing volumes should fall between depths calculated from average and maximum depths. Indeed, for most of the estuaries for which we could find mixing depth data, modeled values fell between these boundaries. Modeled relative mixing depth (f_z) was also found to be positively correlated with DO sensitivity to TN loading (Fig. 6), as would be expected, because increasing relative mixing depth increases the volume for surface production and decreases the volume of the lower layer, where decomposition consumes oxygen.
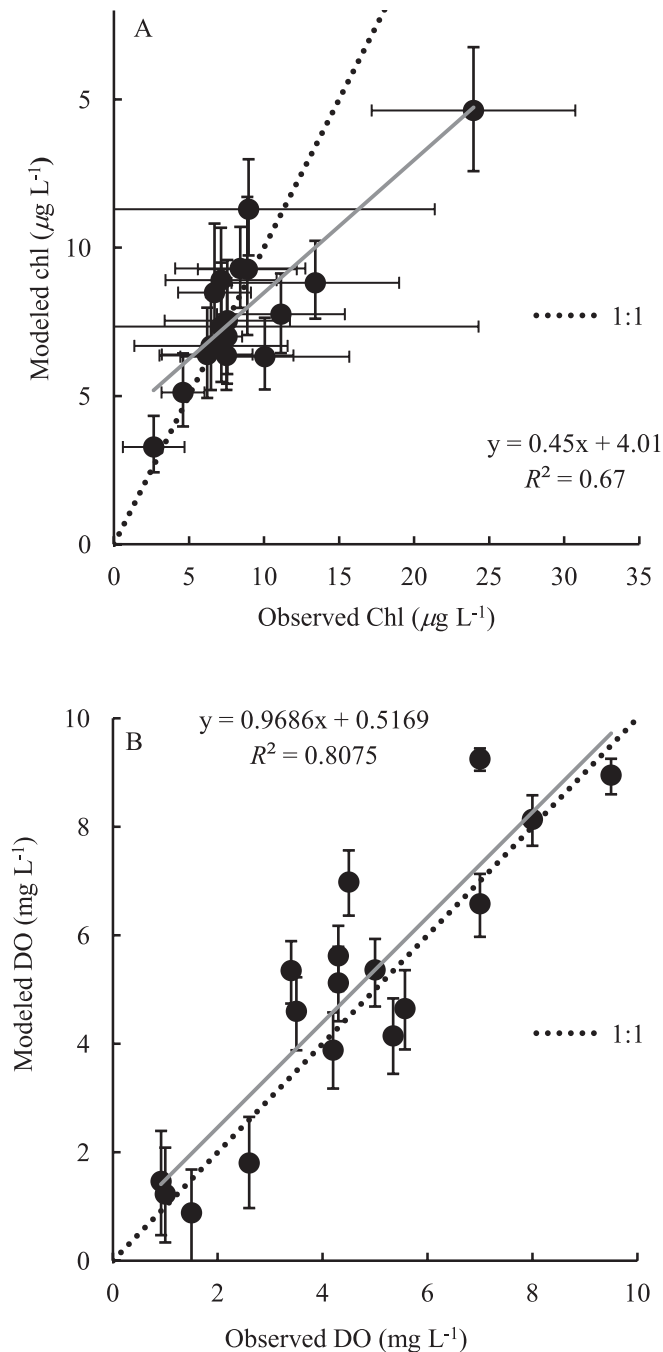

Fig. 4. Model fit for (A) Chl and (B) DO with 95% CI error bars for model predictions and Chl measurements, and parameter α allowed to vary by estuary (fitted and predicted using 1992 SPARROW loads). Regressions of predicted vs. observed are given to summarize model fit; these were calculated using the mean values for each estuary.

Discussion

We used model fitting and parameter analysis to explore the role of estuary eutrophication filters (Cloern 2001) by analyzing a two-layer box model, fit to average estuary Chl and DO concentrations, to test if the sensitivity of DO depletion to TN loads is dependent only on the same
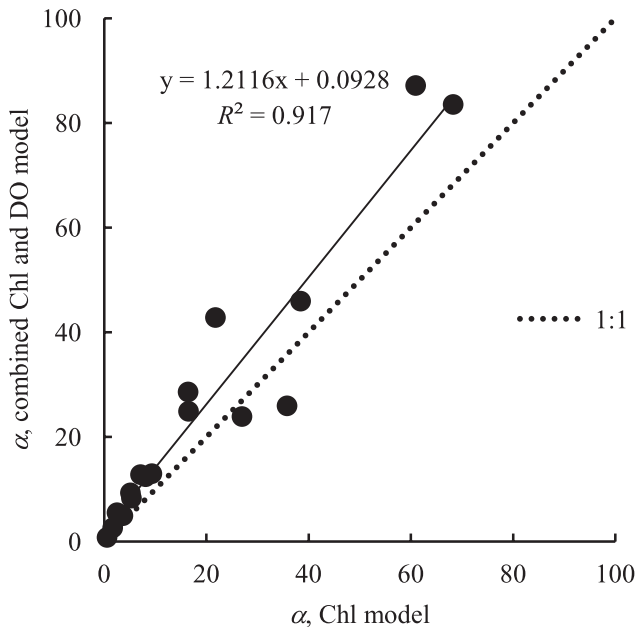
Fig. 5.   Comparison of estuary-specific α values as fit in the Chl model of Scavia and Liu (2009) and as fit using the combined Chl and DO model allowing α and f_z to vary by estuary.

Fig. 6.   DO sensitivity to Chl vs. f_z. Sensitivity of DO drawdown to biomass is defined as (saturated DO − observed DO)/observed Chl.

factors controlling surface Chl or if additional factors are important.

Our calibrations using a single estuary-specific parameter (α, a measure of estuary TN to Chl conversion efficiency, or f_z, relative mixing depth) did not adequately fit the observations. However, allowing both parameters to differ among estuaries worked well, having lower total DIC and fitting both surface Chl and bottom water DO observations; however, this model also tended to overfit the observations, indicating that some statistical noise is also influencing parameter values.

Parameter analysis also showed that DO sensitivity to TN loading was positively correlated with relative mixing depth, suggesting that relative mixing depth acts as a filter on this eutrophication symptom. Our α estimates are similar to those from Scavia and Liu (2009), who also showed that estuary flushing time acts as a filter on Chl concentration.

Sensitivity to TN loading differed among estuaries (i.e., values of α and f_z varied among estuaries). Nutrient loading interacts with other stressors, such as fisheries harvest (Breitburg et al. 2009), to affect various symptoms of eutrophication. Climate variation among estuaries and for a given estuary over time (Duarte et al. 2009) affects water circulation and sensitivity to TN loading. Legacies of past exploitation and nutrient additions can shape estuary response (Duarte et al. 2009). Changes in the ocean-estuary coupling and trophic cascades of San Francisco Bay have increased the efficiency of that system for converting nutrients into algal biomass (Cloern et al. 2007). Water residence time was found to be a primary filter of nutrient effects and a primary predictor of acceptable nutrient loads, defined as the maximum allowable load that would not produce water-quality degregation, in Florida estuaries
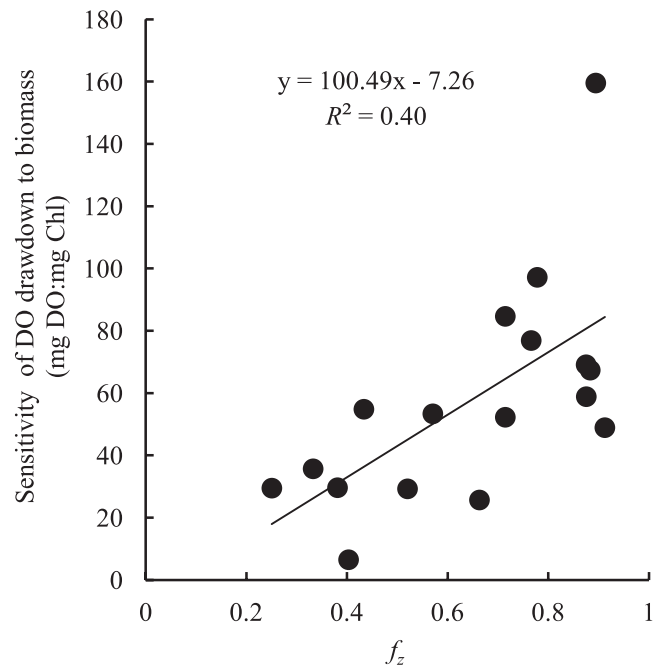
(Steward and Lowe 2010). Our work adds to these findings for individual systems by expanding the geographic and morphological range of systems tested and by including multiple symptoms of eutrophication.

Furthermore, this model and that of Scavia and Liu (2009) show that flushing time and relative mixing depth can be used to estimate the sensitivity of Chl and DO concentrations to TN loading and target potentially sensitive estuaries for further analysis and management.

Flushing time was found to be an indicator of the sensitivity of Chl concentration to TN loads in this model and its predecessor (Scavia and Liu 2009), consistent with other studies (Monbet 1992; Cloern 2001; Steward and Lowe 2010). The effects of biomass removal through flushing are included explicitly in both this and the Scavia and Liu (2009) models; however, additional correlation of flushing time and sensitivity to TN loading, especially in rapidly flushing estuaries, seems to be caused additionally by flushing of nutrients between the spring pulse and summer growth.

Relative mixing depth was found to be an indicator of the sensitivity of DO to TN loading, suggesting that relative mixing depth could be used to classify estuary DO sensitivity. This result is obvious at the extremes. That is, both shallow, well-mixed systems ($f_z \sim 1$) and deep but periodically mixed systems are not prone to seasonal DO depletion. At the other extreme, systems with thick sub-pycnocline regions but extremely limited mixing, for instance, chemically stratified meromictic lakes and fjords, can become hypoxic, but only after years or decades of stratification. However, our analysis suggests that even within a narrower range of relative mixing depths, sensitivity of DO depletion is positively related to relative
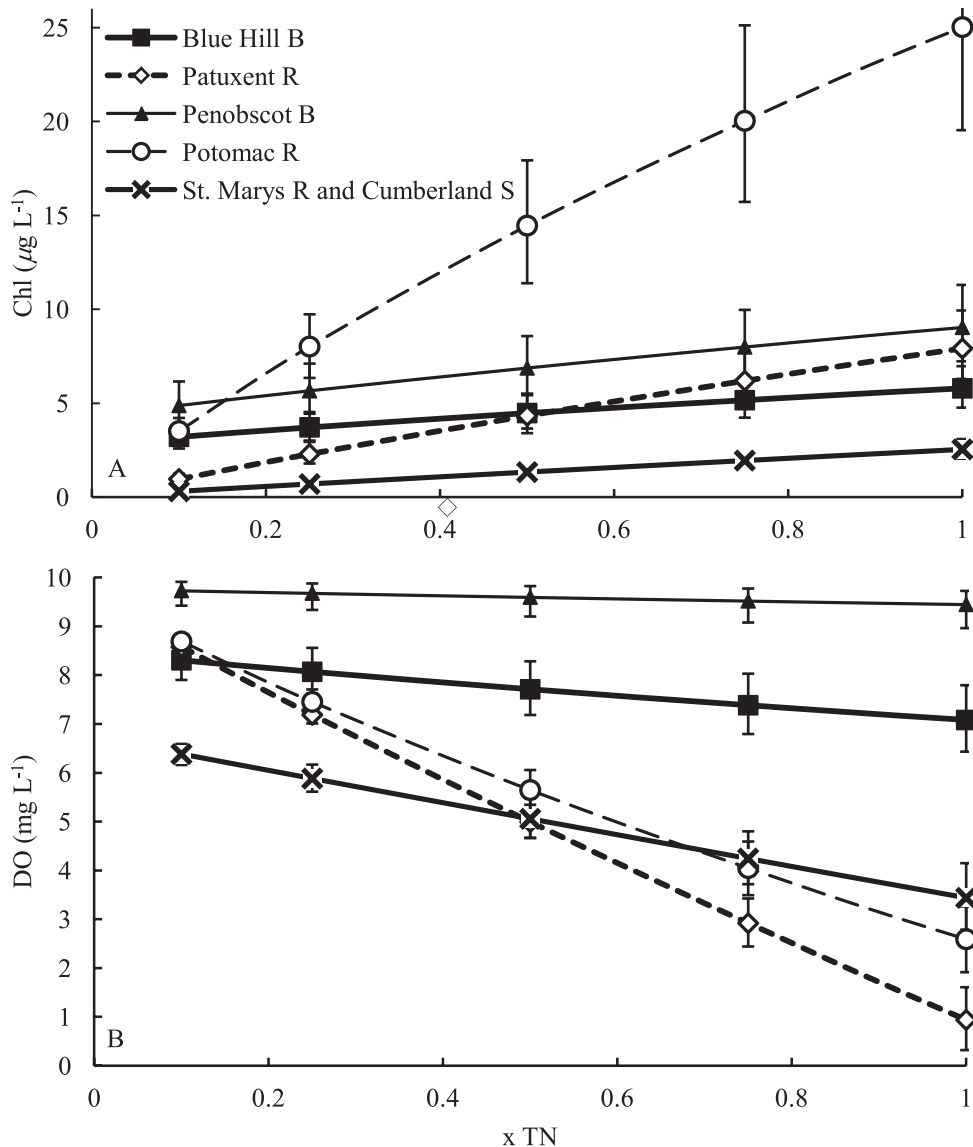
Fig. 7. Forecasting curves for effects of TN loading changes on (A) Chl and (B) DO (mean and 95% CI) for selected estuaries demonstrating the full range of sensitivity to relative TN loading. The *x*-axis shows river TN load relative to the 1992 SPARROW TN load for each estuary. In the figure legend, R = river, B = bay, and S = sound.

mixing depth. Thus, outside of this model calibration, WRT and relative mixing depth can be applied as indicators of estuary sensitivity to target potentially sensitive estuaries for further analysis and management.

Finally, we developed response curves of Chl and DO as a function of TN loads for each of the estuaries included in this study. Examples are shown for a subset that covers the full range of Chl and DO sensitivity to TN loading (Fig. 7). Generating response curves for additional estuaries would require recalibration of this model; however the required data for this (estuary volume, depth, WRT, TN load, river discharge, precipitation and evaporation at the estuary surface, estuary and ocean salinity, and summer surface Chl and bottom water DO) are not difficult to obtain.

Though we focused only on two symptoms of estuary eutrophication, Chl and bottom water DO, these are

important candidates for initial assessments of estuary sensitivity because they are central indicators of other aspects of eutrophication. For example, high Chl is an indicator of high phytoplankton biomass, which can cause decreased light penetration and decreased benthic production and sea grass loss, and low bottom water DO is a driver of fish and shellfish mortality or habitat shifts (Cloern 2001; Rabalais and Turner 2001).

Quantification of the role of physical filters on the sensitivity of estuarine eutrophication to nutrient loading is critical for management in the face of increasing human pressure in coastal areas. Both the comparative information on estuary sensitivity provided by the model and the estuary-specific response curves (e.g., Fig. 7) provide insight into sensitivity of Chl and DO for individual estuaries. Extensive ecological data and more complex

models are available for some U.S. and European estuaries; however, for many hypoxic areas in the developing world (Diaz and Rosenberg 2008), data and models are more limited. Our relatively simple model is well suited to initial screening of such systems.

References

ALEXANDER, R. B., R. A. SMITH, G. E. SCHWARZ, E. W. BOYER, J. V. NOLAN, AND J. W. BRAKEBILL. 2008. Differences in phosphorus and nitrogen delivery to the Gulf of Mexico from the Mississippi River basin. Environ. Sci. Technol. **42:** 822–830, doi:10.1021/es0716103

ATKINSON, M. J., T. BERMAN, B. R. ALLANSON, AND J. IMBERGER. 1987. Fine-scale oxygen variability in a stratified estuary—patchiness in aquatic environments. Mar. Ecol. Prog. Ser. **36:** 1–10, doi:10.3354/meps036001

BLAKE, R. E., AND J. E. DUFFY. 2010. Grazer diversity affects resistance to multiple stressors in an experimental seagrass ecosystem. Oikos **119:** 1625–1635, doi:10.1111/j.1600-0706.2010.18419.x

BORSUK, M. E., C. A. STOW, R. A. LUETTICH, H. W. PAERL, AND J. L. PINCKNEY. 2001. Modelling oxygen dynamics in an intermittently stratified estuary: Estimation of process rates using field data. Estuar. Coast. Shelf. Sci. **52:** 33–49, doi:10.1006/ecss.2000.0726

BREITBURG, D. L., D. W. HONDORP, L. A. DAVIAS, AND R. J. DIAZ. 2009. Hypoxia, nitrogen, and fisheries: Integrating effects across local and global landscapes. Ann. Rev. Mar. Sci. **1:** 329–349, doi:10.1146/annurev.marine.010908.163754

BRICKER, S. B., C. G. CLEMENT, D. E. PIRHALLA, S. P. ORLANDO, AND D. R. G. FARROW. 1999. National estuarine eutrophication assessment: Effects of nutrient enrichment in the nation's estuaries. NOAA, National Ocean Service, Special Projects Office and the National Centers for Coastal Ocean Science.

———, B. LONGSTAFF, W. DENNISON, A. JONES, K. BOICOURT, C. WICKS, AND J. WOERNER. 2007. Effects of nutrient enrichment in the nation's estuaries: A decade of change. NOAA Coastal Ocean Program Decision Analysis Series No. 26; National Centers for Coastal Ocean Science.

CAFFREY, J. M., J. E. CLOERN, AND C. GRENZ. 1998. Changes in production and respiration during a spring phytoplankton bloom in San Francisco Bay, California, USA: Implications for net ecosystem metabolism. Mar. Ecol. Prog. Ser. **172:** 1–12, doi:10.3354/meps172001

CHAPRA, S. C. 1997. Surface water-quality modeling. McGraw-Hill.

CLOERN, J. E. 2001. Our evolving conceptual model of the coastal eutrophication problem. Mar. Ecol. Prog. Ser. **210:** 223–253, doi:10.3354/meps210223

———, A. D. JASSBY, J. K. THOMPSON, AND K. A. HIEB. 2007. A cold phase of the East Pacific triggers new phytoplankton blooms in San Francisco Bay. Proc. Natl. Acad. Sci. USA **104:** 18561–18565, doi:10.1073/pnas.0706151104

DETTMANN, E. H. 2001. Effect of water residence time on annual export and denitrification of nitrogen in estuaries: A model analysis. Estuaries **24:** 481–490, doi:10.2307/1353250

DIAZ, R. J., AND R. ROSENBERG. 2008. Spreading dead zones and consequences for marine ecosystems. Science **321:** 926–929, doi:10.1126/science.1156401

DUARTE, C. M., D. J. CONLEY, J. CARSTENSEN, AND M. SANCHEZ-CAMACHO. 2009. Return to neverland: Shifting baselines affect eutrophication restoration targets. Estuar. Coast. **32:** 29–36, doi:10.1007/s12237-008-9111-2

FENNEL, K., AND E. BOSS. 2003. Subsurface maxima of phytoplankton and chlorophyll: Steady-state solutions from a simple model. Limnol. Oceanogr. **48:** 1521–1534, doi:10.4319/lo.2003.48.4.1521

GELMAN, A., AND J. HILL. 2007. Data analysis using regression and multilevel/hierarchical models. Cambridge Univ. Press.

———, X.-L. MENG, AND H. STERN. 1996. Posterior predictive assessment of model fitness via realized discrepancies. Stat. Sin. **6:** 733–787.

GREENE, R. M., J. C. LEHRTER, AND J. D. HAGY. 2009. Multiple regression models for hindcasting and forecasting midsummer hypoxia in the Gulf of Mexico. Ecol. Appl. **19:** 1161–1175, doi:10.1890/08-0035.1

GRONEWOLD, A. D., S. S. QIAN, R. L. WOLPERT, AND K. H. RECKHOW. 2009. Calibrating and validating bacterial water quality models: A Bayesian approach. Water Res. **43:** 2688–2698, doi:10.1016/j.watres.2009.02.034

HOOKER, S. B., AND E. R. FIRESTONE [EDS.]. 2003. Algorithm updates for the fourth SeaWiFS data reprocessing. NASA Goddard Space Flight Center.

HOWARTH, R. W., AND R. MARINO. 2006. Nitrogen as the limiting nutrient for eutrophication in coastal marine ecosystems: Evolving views over three decades. Limnol. Oceanogr. **51:** 364–376, doi:10.4319/lo.2006.51.1_part_2.0364

HULL, V., L. PARRELLA, AND M. FALCUCCI. 2008. Modelling dissolved oxygen dynamics in coastal lagoons. Ecol. Model. **211:** 468–480, doi:10.1016/j.ecolmodel.2007.09.023

KEMP, W. M., E. M. SMITH, M. MARVIN-DIPASQUALE, AND W. R. BOYNTON. 1997. Organic carbon balance and net ecosystem metabolism in Chesapeake Bay. Mar. Ecol. Prog. Ser. **150:** 229–248, doi:10.3354/meps150229

———, AND OTHERS. 2005. Eutrophication of Chesapeake Bay: Historical trends and ecological interactions. Mar. Ecol. Prog. Ser. **303:** 1–29, doi:10.3354/meps303001

LIU, Y., M. A. EVANS, AND D. SCAVIA. 2010. Gulf of Mexico hypoxia: Exploring increasing sensitivity to nitrogen loads. Environ. Sci. Technol. **44:** 5836–5841, doi:10.1021/es903521n

———, AND D. SCAVIA. 2010. Analysis of the Chesapeake Bay hypoxia regime shift: Insights from two simple mechanistic models. Estuar. Coast. **33:** 629–639, doi:10.1007/s12237-009-9251-z

LUCAS, L. V., J. E. CLOERN, J. R. KOSEFF, S. G. MONISMITH, AND J. K. THOMPSON. 1998. Does the Sverdrup critical depth model explain bloom dynamics in estuaries? J. Mar. Res. **56:** 375–415, doi:10.1357/002224098321822357

LUNN, D. J., A. THOMAS, N. BEST, AND D. SPIEGELHALTER. 2000. Winbugs—a Bayesian modeling framework: Concepts, structure, and extensibility. Stat. Comput. **10:** 325–337, doi:10.1023/A:1008929526011

MALVE, O., AND S. S. QIAN. 2006. Estimating nutrients and chlorophyll *a* relationships in Finnish lakes. Environ. Sci. Technol. **40:** 7848–7853, doi:10.1021/es061359b

MONBET, Y. 1992. Control of phytoplankton biomass in estuaries—a comparative analysis of microtidal and macrotidal estuaries. Estuaries **15:** 563–571, doi:10.2307/1352398

Murrell, M. C., J. G. Campbell, J. D. Hagy, and J. M. Caffrey. 2009. Effects of irradiance on benthic and water column processes in a Gulf of Mexico estuary: Pensacola Bay, Florida, USA. Estuar. Coast. Shelf. Sci. **81:** 501–512, doi:10.1016/j.ecss.2008.12.002

Park, K., C. K. Kim, and W. W. Schroeder. 2007. Temporal variability in summertime bottom hypoxia in shallow areas of Mobile Bay, Alabama. Estuar. Coast. **30:** 54–65.

Qian, S. S., C. A. Stow, and M. E. Borsuk. 2003. On Monte Carlo methods for Bayesian inference. Ecol. Model. **159:** 269–277, doi:10.1016/S0304-3800(02)00299-5

Rabalais, N. N., and R. E. Turner. 2001. Coastal hypoxia: Consequences for living resources and ecosystems. American Geophysical Union.

Renaud, M. L. 1986. Hypoxia in Louisiana coastal waters during 1983—implications for fisheries. Fish. Bull. **84:** 19–26.

Riemann, B., P. Simonsen, and L. Stensgaard. 1989. The carbon and chlorophyll content of phytoplankton from various nutrient regimes. J. Plankton. Res. **11:** 1037–1045, doi:10.1093/plankt/11.5.1037

Scavia, D., E. L. A. Kelly, and J. D. Hagy. 2006. A simple model for forecasting the effects of nitrogen loads on Chesapeake Bay hypoxia. Estuar. Coast. **29:** 674–684.

———, and Y. Liu. 2009. Exploring estuarine nutrient susceptibility. Environ. Sci. Technol. **43:** 3474–3479, doi:10.1021/es803401y

Scully, M. E. 2010. The importance of climate variability to wind-driven modulation of hypoxia in Chesapeake Bay. J. Phys. Oceanogr. **40:** 1435–1440, doi:10.1175/2010JPO4321.1

Sharples, J., M. J. Coates, and J. E. Sherwood. 2003. Quantifying turbulent mixing and oxygen fluxes in a Mediterranean-type, microtidal estuary. Ocean. Dynam. **53:** 126–136, doi:10.1007/s10236-003-0037-8

Spiegelhalter, D. J., N. G. Best, B. R. Carlin, and A. Van Der Linde. 2002. Bayesian measures of model complexity and fit. J. Roy. Stat. Soc. B, Stat Meth **64:** 583–616, doi:10.1111/1467-9868.00353

Steward, J. S., and E. F. Lowe. 2010. General empirical models for estimating nutrient load limits for Florida's estuaries and inland waters. Limnol. Oceanogr. **55:** 433–445, doi:10.4319/lo.2010.55.1.0433

Swaney, D. P., D. Scavia, R. W. Howarth, and R. M. Marino. 2008. Estuarine classification and response to nitrogen loading: Insights from simple ecological models. Estuar. Coast. Shelf. Sci. **77:** 253–263, doi:10.1016/j.ecss.2007.09.013

Turner, R. E., N. N. Rabalais, and D. Justić. 2008. Gulf of Mexico hypoxia: Alternate states and a legacy. Environ. Sci. Technol. **42:** 2323–2327, doi:10.1021/es071617k

Weiss, R. F. 1970. Solubility of nitrogen, oxygen and argon in water and seawater. Deep-Sea Res. **17:** 721–735.

Wiley, M. J., and others. 2010. A multi-modeling approach to evaluating climate and land use change impacts in a Great Lakes river basin. Hydrobiologia **657:** 243–262, doi:10.1007/s10750-010-0239-2

Zhang, J., and others. 2010. Natural and human-induced hypoxia and consequences for coastal areas: Synthesis and future development. Biogeosciences **7:** 1443–1467, doi:10.5194/bg-7-1443-2010